Chapter 4

Molecular freeze-out as a tracer of the thermal and dynamical evolution of pre- and protostellar cores

Abstract

Radiative transfer models of multi-transition observations are used to determine molecular abundances as functions of position in pre- and protostellar cores. The data indicate a "drop" abundance profile with radius, with high abundances in the outermost regions probed by low excitation 3 mm lines, and much lower abundances at intermediate zones probed by higher frequency lines. The results are illustrated by fits to the CO, HCO^+ and N_2H^+ lines for a subset of objects. We propose a scenario in which the molecules are frozen out in a region of the envelope where the temperature is low enough ($\lesssim$ 40 K) to prevent immediate desorption, but where the density is high enough ($>10^4$–10^5 cm^{-3}) that the freeze-out timescales are shorter than the lifetime of the core. The size of the freeze-out zone is thereby a record of the thermal and dynamical evolution of the cores. Fits to data for a sample of 18 objects indicate that the size of the freeze-out zone decreases significantly between Class 0 and I objects, explaining the variations in, for example, CO abundances with envelope masses. However, the corresponding timescales are $10^{5\pm0.5}$ years, with no significant difference between Class 0 and I objects. These timescales indicate that the dense pre-stellar phase with heavy depletions lasts only a short time, $\leq 10^5$ yr.

Jørgensen, Schöier & van Dishoeck, 2004, A&A, submitted

4.1 Introduction

The environments of the youngest pre- and protostellar objects are characterized by large amounts of cold gas and dust. The chemistry in these early stages is affected to a large degree by freeze-out of molecules onto dust grains (e.g., Bergin & Langer 1997) and is thus closely linked to the thermal evolution of the cores. An important question is how the pre- and protostellar stages are linked and what their respective timescales are. In the pre-stellar stages the thermal balance is dominated by the external radiation field, which, except in special cases, does not heat the material to temperatures higher than ≈ 15 K (e.g., Evans et al. 2001). At such low temperatures most molecules gradually freeze out, with very short timescales in the innermost dense regions and increasing timescales toward the exterior where they may become longer than the age of the core (e.g., Caselli et al. 1999).

In the protostellar stages, in contrast, the thermal balance is dominated by the heating from the central newly formed protostar, introducing a steep tem-

perature gradient toward the core center. Radiative transfer modeling of the dust continuum emission shows that the characteristic temperatures can rise to a few hundred K in the innermost regions (e.g., Ivezić & Elitzur 1997; Shirley et al. 2002). Still, significant depletions are observed also in these stages, e.g., for CO, indicating that a substantial fraction of the envelope material remains at low temperatures (e.g., Blake et al. 1995; Ceccarelli et al. 2001). In a large survey of pre- and protostellar objects, Jørgensen et al. (2002, 2004d) found a strong correlation between the abundances of CO (and related species such as HCO^+) and envelope mass.

The timescales for freeze-out and evaporation depend sensitively on density and temperature. The availability of accurate physical structures from dust continuum data thus provides an opportunity to constrain the timescales independently using only chemistry. Currently, the ages of pre- and protostellar objects are determined almost exclusively from statistics, such as the number counts of cores with and without associated far-infrared (IRAS) sources (e.g., Lee & Myers 1999; Jessop & Ward-Thompson 2000), resulting in a large spread in pre-stellar ages from $\sim 10^5$ to a few $\times 10^6$ yr. Our semi-empirical procedure for constraining the chemistry and its assumptions are summarized in Fig. 1 of Doty et al. (2004), and consists in the simplest case of fitting a constant abundance to the data, as used in our previous papers. In this Letter, we introduce a "drop" abundance profile with a specific "freeze-out" region with low abundances, and we relate the size and location of this depletion zone to pre- and protostellar evolution. This study is also an important complement to full chemo-hydrodynamical models which follow the chemistry in time as the matter collapses to form a central star (e.g., Rawlings et al. 1992; Lee et al. 2004).

4.2 Model

The main assumption in our analysis is that the chemical structure in the protostellar stages is controlled by thermal desorption processes. Although other non-thermal processes such as cosmic-ray induced desorption play a role for weakly-bound species like CO, they cannot prevent freeze-out in the densest and coldest gas (e.g., Shen et al. 2004). Similarly, photodesorption can keep molecules off the grains, but this only involves the outermost regions up to an $A_V \approx 2$ (Bergin et al. 1995). These effects are expected to be secondary to the abundance structure resulting from the freeze-out and thermal evaporation of CO. Finally, outflows and shocks may be important in regulating the abundance structures, but the narrow line-widths for optically thin species such as $C^{18}O$ and $H^{13}CO^+$ suggest that they probe predominantly the quiescent bulk envelope material. Our analysis focusses on the chemistry in the outer envelope on 500–10,000 AU scales, and does not consider the additional abundance jumps in the innermost region (<100 AU) at $T > 100$ K where all ices evaporate.

Following Rodgers & Charnley (2003), the thermal desorption rate ξ and

the freeze-out rate λ can be calculated from

$$\xi(\mathrm{M}) = \nu(\mathrm{M})\ \exp\left(-\frac{E_\mathrm{b}(\mathrm{M})}{kT_\mathrm{d}}\right) \qquad [\mathrm{s}^{-1}] \tag{4.1}$$

$$\lambda(\mathrm{M}) = 4.55\times10^{-18}\left(\frac{T_\mathrm{g}}{m(\mathrm{M})}\right)^{0.5} n_\mathrm{H} \qquad [\mathrm{s}^{-1}] \tag{4.2}$$

where $\nu(\mathrm{M})$ is the vibrational frequency of the considered molecule M in its binding site in the ice mantle, T_d and T_g the dust and gas temperatures, respectively, $m(\mathrm{M})$ the molecular weight, and n_H the total hydrogen density. $E_\mathrm{b}(\mathrm{M})$ is the binding energy of the molecule depending on the ice mantle composition, for which we adopt the values tabulated by Aikawa et al. (1997). Fig. 4.1 shows the desorption and freeze-out timescales, defined as $1/\xi(\mathrm{M})$ and $1/\lambda(\mathrm{M})$, respectively, as functions of depth for two protostars from the sample of Jørgensen et al. (2002), NGC 1333-IRAS2 and TMR1. These objects are classified as Class 0 and I, and have significantly different envelope masses of 1.7 and 0.12 $\mathrm{M}_\odot$, respectively. Their temperatures and densities have been constrained from submillimeter continuum data and vary strongly with radius. Figure 4.1 shows that freeze-out can – for a given age – only occur for a restricted region of density and temperature in the envelope. At high temperatures $T > T_\mathrm{ev}$ the molecule evaporates whereas at low densities $n < n_\mathrm{de}$ the freeze-out timescale is too long. Due to the exponential dependence in Eq. (4.1), the thermal desorption proceeds very rapidly as soon as the temperature is higher than T_ev. In contrast, the freeze-out timescale varies more slowly with depth in the envelope, due to the inverse dependence on density.

In order to quantify this scenario, a "drop" abundance structure is introduced as a trial profile, with a depleted abundance X_D where $T \leq T_\mathrm{ev}$ and $n \geq n_\mathrm{de}$, and an undepleted abundance X_0 where $T \geq T_\mathrm{ev}$ or $n \leq n_\mathrm{de}$. Whereas T_ev is in principle a well-defined quantity depending primarily on the ice mantle properties, n_de depends on the lifetime of the core compared to the depletion timescale (induced in the pre- and protostellar stages) and the dynamical evolution of the core at earlier stages, including replenishment of undepleted material through infall from larger radii. For this discussion we only assume step functions at T_ev and n_de, which are thus free parameters together with X_0 and X_D. Single-dish data on CO, HCO^+, and N_2H^+ taken from Jørgensen et al. (2004d) are fitted for four objects at different stages of evolution. For the HCO^+ and N_2H^+ fits, T_ev and n_de are taken from the fits to the CO data, giving low values of the χ^2-estimator.

The best fit parameters are listed in Table 4.1 and illustrated in Fig. 4.2. For the class I object, the data are found to be consistent with a model without a depletion zone. For CO and HCO^+, X_0 is found to be nearly identical for all sources, with X_D typically an order of magnitude lower than X_0. For CO, X_0 is found to be 2.7×10^{-4} consistent with the results of Lacy et al. (1994). N_2H^+ shows the opposite behavior, since its abundance is enhanced when CO is frozen out (e.g., Bergin & Langer 1997; Jørgensen et al. 2004d). For NGC 1333-IRAS2 and L723, no constraints are available on X_0 for N_2H^+ in the outermost

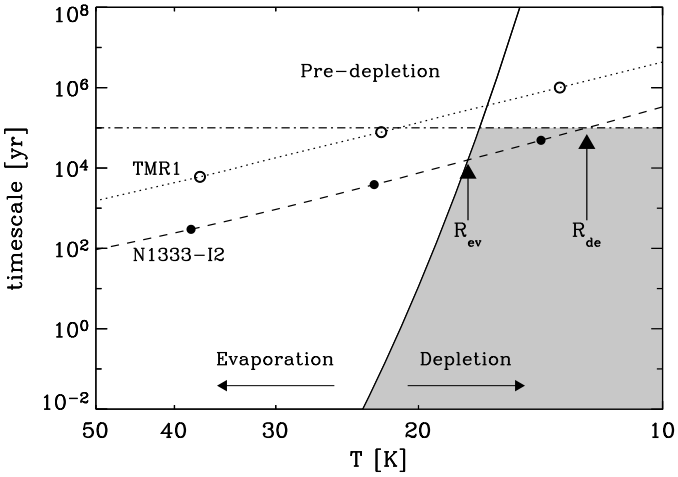

Figure 4.1. *Comparison between CO desorption and freeze-out timescales as functions of temperature and density. The solid line indicates the desorption timescale while the dotted and dashed lines indicate the (density and temperature dependent) freeze-out timescales for TMR1 and N1333-I2, respectively. Depletion occurs where the curves for the freeze-out timescale intersect the colored region, in this example for an assumed age of 10^5 years (dash-dotted line). Freeze-out timescales corresponding to H_2 densities of $1{\times}10^5$, $1{\times}10^6$ and $1{\times}10^7$ cm^{-3} for NGC 1333-IRAS2 and $1{\times}10^4$, $1{\times}10^5$ and $1{\times}10^6$ cm^{-3} for TMR1 have been indicated by the filled and open circles, respectively.*

part. The CO evaporation temperatures $T_{\rm ev}$ are all found to be ≥ 35 K, consistent with the results of Jørgensen et al. (2002). The derived abundance profile depends somewhat on the adopted outer radius and any contribution from the surrounding cloud to the lowest excitation lines. However, the drop abundance profiles are also necessary to reproduce higher angular resolution interferometer data, where contributions from the larger scale cloud are resolved out, as well as transitions with higher critical densities of H_2CO and HCO^+ (Schöier et al. 2004a; Jørgensen 2004, and Table 4.1).

Given the success of these models, the $C^{18}O$ and $C^{17}O$ lines for the entire sample of Jørgensen et al. (2002) have been fitted assuming an undepleted abundance X_0 of $2.7{\times}10^{-4}$ and an evaporation temperature, $T_{\rm ev}$, of 35 K. For each source, all lines could be well fitted ($\chi^2_{\rm red} \leq 2$) using depletion densities $n_{\rm de}$ =$1{\times}10^4$–$6{\times}10^5$ cm^{-3} ($10^{5\pm0.4}$ cm^{-3}) corresponding to depletion timescales of 2×10^4–8×10^5 years ($10^{5\pm0.5}$ years). No significant difference in timescales between Class 0 and I objects is found. For the objects with the least massive envelopes ($M \lesssim 0.1\ M_\odot$) where photodesorption could become an issue, the derived $t_{\rm de}$ is a lower limit to the actual depletion timescale. In general for our objects, however, the depletion radius is located further in the envelope than

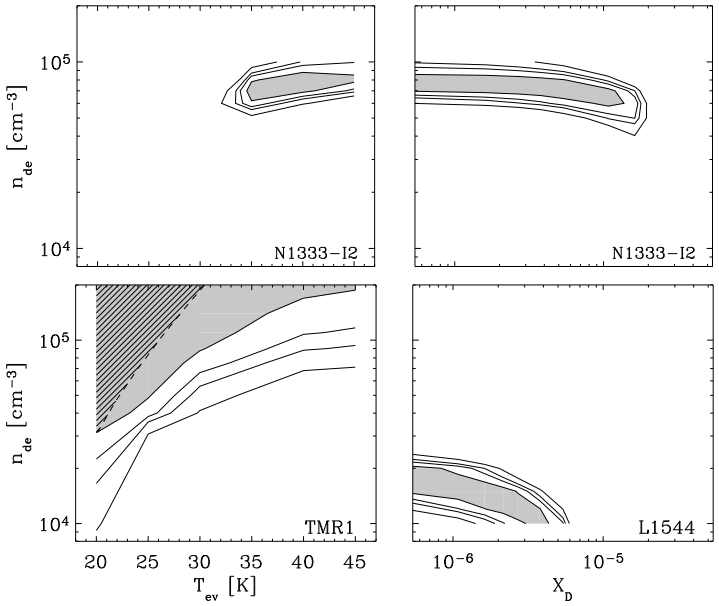

Figure 4.2. *χ^2 confidence plots for fits to the CO lines toward NGC 1333-IRAS2 (upper panels) and TMR1 and L1544 (lower left and right panels, respectively). In each plot the grey area marks the 1σ confidence region and the subsequent line contours the 2σ, 3σ and 4σ confidence regions. In the lower left panel the dashed region indicates constant abundance models (i.e., for such high $n_{\rm de}$/low $T_{\rm ev}$ that the drop region is non-existent).*

the radius where $A_{\rm V} = 2$.

4.3 Discussion

The fact that the drop abundance profiles fit all sources and molecules studied shows that this structure provides a good representation of the dominant chemistry in protostellar envelopes, with all other chemical effects being of secondary importance. Fig. 4.3 compares the radii corresponding to $T_{\rm ev}$ and $n_{\rm de}$ for varying envelope masses for a 3 $L_\odot$ central source. For an object with a large envelope mass like NGC 1333-IRAS2, the depletion zone is a few thousand AU, a substantial fraction of the entire envelope. Progressive dispersion and heating decreases the size of the depleted region as the evaporation radius moves outward until it becomes vanishingly small, as in the case of TMR1. This indicates that the trend of (constant) abundances increasing with decreasing envelope mass for these species (Jørgensen et al. 2002, 2004d) reflects the size of the depletion region.

Based on the above fits, we propose a chemical structure of the outer en-

Table 4.1. *Best fit parameters for CO, HCO^+ and N_2H^+ lines for the protostars N1333-I2, L723, TMR1 and the pre-stellar core L1544.*

	N1333-I2	L723	TMR1	L1544
$T_{\rm ev}$ [K]	$\gtrsim$ 35	40	...	...
$n_{\rm de}$ [10^4 cm^{-3}]	7	4	...	1.5
CO:				
X_0 [10^{-4}]	2.7	2.7	2.7	2.7
$X_{\rm D}$ [10^{-4}]	<0.14	0.14	...	0.016
χ^2 / N	4.4 / 7	2.4 / 6	0.75 / 6	4.2 / 4
HCO^+:				
X_0 [10^{-8}]	1.8	<2.0	2.7[b]	–
$X_{\rm D}$ [10^{-8}]	0.26	0.35	...	–
χ^2 / N	4.1 / 5	1.8 / 3	2.1[b] / 2	–
N_2H^+:				
X_0 [10^{-9}]	?	?	0.35	–
$X_{\rm D}$ [10^{-9}]	5.0	1.3	...	–
$t_{\rm de}$ [10^5 yrs][a]	2	3	$\lesssim$ 1[c]	8

Notes: The abundances have been derived from observations of the optically thin isotopic species, $C^{18}O$, $C^{17}O$ and $H^{13}CO^+$ assuming the standard isotopic ratios adopted in Jørgensen et al. (2004d). [a]Depletion timescale corresponding to the derived $n_{\rm de}$ using Eq. (4.2). [b]Model including excitation through collisions with electrons at densities $\leq 3 \times 10^4$ cm^{-3}. [c]1σ limit assuming $T_{\rm ev}$ of 35 K.

velopes as shown schematically in Fig. 4.4. The main difference between the pre- and protostellar cores is the inner source of heating in the protostars that causes CO to be evaporated rather than depleted toward the source center. The main difference between the Class 0 and I objects is the size of the depletion zone.

Is this chemical structure also an evolutionary indicator? In contrast with the size of the depletion zone, no clear correlation is seen between the derived age $t_{\rm de}$ and derived envelope mass or luminosity for the entire sample (e.g., Table 1). This indicates that the depletion timescales must also reflect other properties, such as the mass of the core from which the protostar is formed. The relatively short timescales of $10^{5\pm0.5}$ years suggest that the depletion structure is established in the pre-stellar stages, but only after the pre-stellar core has become dense enough that freeze-out really sets in. The rather small scatter seen indicates that this stage is short, $\lesssim 10^5$ years.

This timescale provides an interesting independent age constraint for the

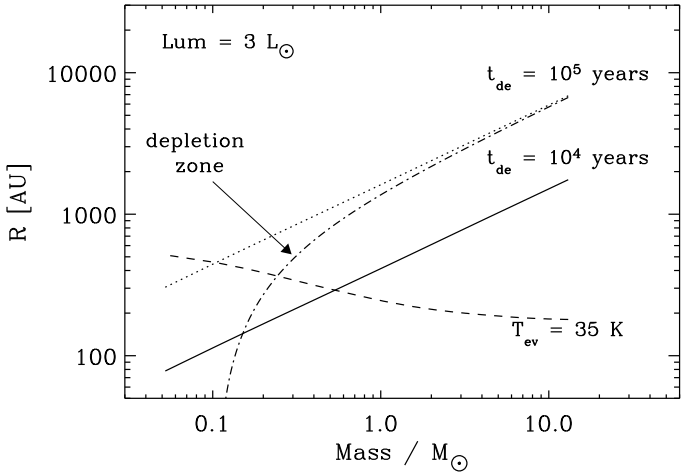

Figure 4.3. *Characteristic radii as functions of envelope mass for a 3 $L_\odot$ protostar using the models of Jørgensen et al. (2002). An $n \propto r^{-1.5}$ envelope density profile was assumed with inner and outer radii of 25 and 15000 AU, respectively. The dashed line indicate the radius where $T_{\rm ev} = 35$ K and the solid and dotted lines the radii where the depletion timescales are 10^4 and 10^5 years, respectively. The dashed-dotted line indicates the difference between the depletion and evaporation radii (i.e., size of the depletion zone) for a depletion timescale of 10^5 years.*

studies of core collapse, since it is shorter than the ages derived from the above mentioned statistical studies (e.g., Lee & Myers 1999; Jessop & Ward-Thompson 2000). This apparent discrepancy may reflect simply the definition of the pre-stellar stage: our estimate refers only to the dense pre-stellar where depletion has become significant. On the other hand, the statistical studies may be missing low-luminosity embedded infrared sources due to the limited sensitivty of IRAS (see, e.g., Young et al. 2004) and thus lead to overestimates of the timescales. Further unbiased surveys, e.g., with the Spitzer Space Telescope, may shed further light into this issue.

To refine the proposed models, it will be necessary to couple models for the dynamical and radial chemical evolution to fully address the use of $n_{\rm de}$ as a tracer of age (Lee et al. 2004). On the other hand, since the dynamical structure of protostellar cores is often inferred from fits of line profiles of molecules such as HCO^+ (e.g., Gregersen et al. 1997), knowledge about the radial chemical structure is important for detailed descriptions of the infalling envelope. For example, the location of the collapse radius in the inside-out collapse model for the envelope around NGC 1333-IRAS2 (Jørgensen et al. 2004b) is at ≈ 1000 AU which is in the middle of the drop zone where the temperature is ≈ 25 K. The exact "infall" line profile will therefore depend critically not only on the

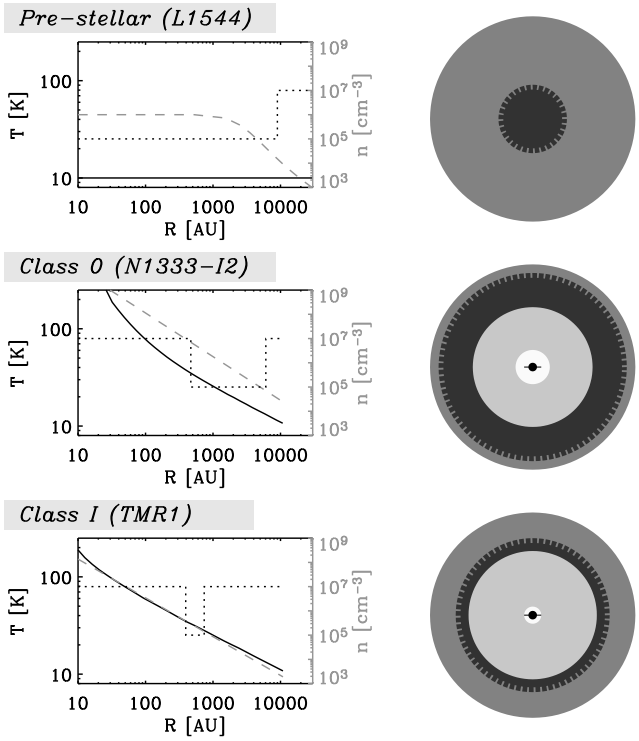

Figure 4.4. *Proposed chemical evolutionary sequence for low-mass pre- and protostellar objects. The left column gives the temperature and density as functions of radius (black solid and grey dashed lines, respectively) for three archetypical low-mass pre- and protostellar objects: L1544 (pre-stellar core), N1333-I2 (class 0, $M_{\rm env} > 0.5\,M_\odot$ protostar) and TMR1 (class I, $M_{\rm env} < 0.5\,M_\odot$ protostar). The black dotted line indicate the derived abundance structure. The right column gives the depletion signature for each class of object with, going from the outside to the inside, the dark grey indicating the region where the density is too low for depletion ($n < n_{\rm de}$), the black indicating the region where the molecules deplete and the light grey indicating the region where they evaporate ($T > T_{\rm ev}$).*

velocity field but also the presence and location of the outer pre-depletion ($n < n_{\rm de}$) zone and the amount of depletion.

Acknowledgements

The authors thank Ted Bergin, Jeong-Eun Lee and Neal Evans for useful discussions. The research of JKJ is made possible through a NOVA network 2 Ph.D. stipend, FLS acknowledges support from the Swedish Research Council. Astrochemistry research in Leiden is supported by a NWO Spinoza grant.